European Journal of Mechanics B/Fluids 29 (2010) 465–471

Contents lists available at ScienceDirect

European Journal of Mechanics B/Fluids

journal homepage: www.elsevier.com/locate/ejmflu

Navier–Stokes solutions for steady parallel-sided pendent rivulets

Andrés Jorge Tanasijczuk [a], Carlos Alberto Perazzo [b,*,1], Julio Gratton [c,1]

[a] Universidad de Buenos Aires, Buenos Aires, Argentina

[b] Dto. de Física y Química, Universidad Favaloro, Solís 453, 1078, Buenos Aires, Argentina

[c] INFIP–CONICET, Dto. de Física, Facultad de Ciencias Exactas y Naturales, Universidad de Buenos Aires, Ciudad Universitaria, Pab. I, 1428, Buenos Aires, Argentina

ARTICLE INFO

Article history:
Received 6 November 2009
Received in revised form
21 May 2010
Accepted 10 June 2010
Available online 23 June 2010

Keywords:
Navier–Stokes equations
Parallel flow
Pendent rivulet

ABSTRACT

We investigate exact solutions of the Navier–Stokes equations for steady rectilinear pendent rivulets running under inclined surfaces. First we show how to find exact solutions for sessile or hanging rivulets for any profile of the substrate (transversally to the direction of flow) and with no restrictions on the contact angles. The free surface is a cylindrical meniscus whose shape is determined by the static equilibrium between gravity and surface tension, by the shape of the solid surface, and by the contact angles on both contact lines. Given this, the velocity field can be obtained by integrating numerically a Poisson equation. We then perform a systematic study of rivulets hanging below an inclined plane, computing some of their global properties, and discussing their stability.

1. Introduction

Steady parallel flows with a free surface such as rivulets flowing over or under inclined surfaces, flows in inclined channels of various cross sections, etc. are of great interest since they model many natural as well as industrial flows. These currents are driven by gravity, to which in some instances stresses on the free surface (like those arising from wind) must be added. These and the viscous forces determine the velocity field, while the shape of the free surface depends on a balance between surface tension and gravity, and on the contact angles on both contact lines.

The first investigation of the steady unidirectional flow of a uniform rivulet of a Newtonian fluid down an inclined plane is due to Towell and Rothfeld [1]. This work was later extended by many authors. Allen and Biggin [2] addressed rectilinear rivulet flow by means of a series expansion in terms of the rivulet aspect ratio (height/width) and compared the results with an exact numerical solution. Duffy and Moffat [3] calculated the shape of the rivulet as a function of the inclination of the substrate. Non-planar supporting surfaces were considered by Alekseenko et al. [4], who treated flows down the lower surface of an inclined circular cylinder, and by Wilson and Duffy [5] who considered rivulets on a substrate with a slow variation transverse to the direction of flow. Thermocapillary effects on thin viscous rivulets draining down a heated or cooled substrate were also investigated [6], as well as temperature-dependent viscosity effects [7,8]. Rivulet flow of non-Newtonian liquids was considered by Rosenblat [9], and more recently by Wilson et al. [10]. A rivulet driven by interfacial shear and gravity was investigated by Myers et al. [11], as well as by Sullivan et al. [12,13]. Braiding and meandering of rivulets flowing on a partially wetting inclined plane have been addressed by Mertens et al. [14,15] and Birnir et al. [16]. In all these works it is assumed that the thickness of the rivulet varies smoothly. This requires that the aspect ratio be small and that the contact angle be not too large.

In the light of the previous comments it appears that the basic theory of the steady parallel flows with a free surface on an inclined substrate is well known. However in many instances the condition of small free surface slope is violated, so that the above-mentioned theoretical results are, at best, approximate. Exact solutions of the Navier–Stokes equations for these situations have been obtained numerically only for a few particular cases [2,11] and have not yet been investigated systematically. Accurate quantitative solutions that go beyond the known approximate results require extensive computations and their results are not obvious nor trivial but are important for applications, as well as to assess the accuracy of the approximate results that can be found in the literature.

Recently we investigated exact solutions of the Navier–Stokes equations that describe rivulets flowing over an inclined plane, with no limitations on the aspect ratio nor on the contact angle [17]. Here we extend this work to consider exact solutions for steady rectilinear rivulets running over or under inclined surfaces that may have an arbitrary profile transversally to the direction of flow, as well as changes of the wettability across the supporting surface. Given the shape of the rivulet, the velocity field is obtained

* Corresponding author.
E-mail addresses: perazzo@favaloro.edu.ar (C.A. Perazzo), jgratton@tinfip.lfp.uba.ar (J. Gratton).

[1] Researcher of CONICET.

0997-7546/$ – see front matter © 2010 Elsevier Masson SAS. All rights reserved.
doi:10.1016/j.euromechflu.2010.06.002

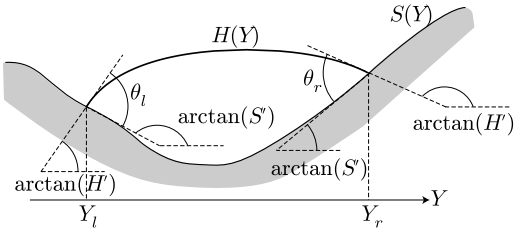

Fig. 1. Geometry of the problem.

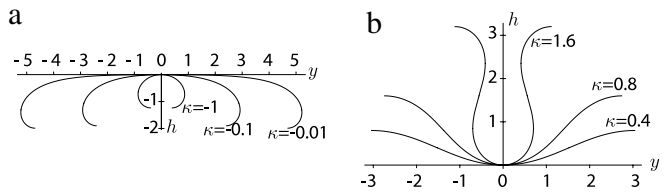

Fig. 2. Solutions (7) for different values of κ for (a) $\sigma = +1$, (b) $\sigma = -1$. Notice that reversing the sign of κ produces a solution with the same y, and h with opposite sign.

by integrating numerically a Poisson equation. We give a few examples of sessile and hanging rivulets. Next we perform a systematic study of rivulets hanging below an inclined plane; we compute their global properties (cross-sectional area, thickness, width of the wetted region, volumetric flow, etc.), and we discuss their stability.

2. The shape of the free surface and the velocity field

The theory of cylindrical menisci was developed long ago [18,1]. Here we cast it in a form that simplifies the task of computing exact solutions for any profile of the substrate, and without limitations on the static contact angles. We consider a rivulet flowing steadily over or under a rigid cylindrical substrate, whose inclination is $\alpha \in [0, \pi]$. The X coordinate is along the cylinder and increases downward, and the Y coordinate is horizontal (Fig. 1). Then X is ignorable and the topography $Z = S(Y)$ of the substrate is a datum. We indicate the free surface with $Z = H(Y)$, the surface tension with γ, the density of the liquid with ρ, and g is the acceleration of gravity. To allow for transversal changes of the wettability we denote the left and right contact angles with θ_l and θ_r. The velocity field is $\boldsymbol{U} = U(Y, Z)\hat{\boldsymbol{X}}$. The boundary condition at the free surface is then

$$\mathsf{T} \cdot \hat{\boldsymbol{n}} = \gamma K \hat{\boldsymbol{n}}, \tag{1}$$

where T is the stress tensor, $K(Y) = H''(1 + H'^2)^{-3/2}$ is the curvature of the free surface (primes denote derivatives with respect to the argument) and $\hat{\boldsymbol{n}}$ is its normal. The z component of the momentum equation is

$$0 = -\frac{\partial P}{\partial Z} - \rho g \cos\alpha, \tag{2}$$

where P is the pressure. The component of Eq. (1) in the normal direction states that $P = -\gamma K$ at $Z = H$, so that the pressure is

$$P = \rho g(H - Z) - \gamma K. \tag{3}$$

The y component of the momentum equation is $0 = -\partial P/\partial Y$. Using this in (3) we obtain the equation that determines the shape of the free surface:

$$\frac{\rho g \cos\alpha}{\gamma} H' = \left[\frac{H''}{(1 + H'^2)^{3/2}}\right]'. \tag{4}$$

This equation can also be obtained by minimization of gravitational plus surface energy.

When $\alpha = \pi/2$ the solution of (4) is a circle. If $\alpha \neq \pi/2$, introducing the factor $\sigma = +1$ for sessile rivulets ($0 \leq \alpha < \pi/2$) and $\sigma = -1$ for hanging rivulets ($\pi/2 < \alpha \leq \pi$), defining the capillary length $\lambda = \sqrt{\gamma/\rho g|\cos\alpha|}$, and using the dimensionless variables $h = H/\lambda$, $y = Y/\lambda$, we can write (4) as

$$\sigma h' = \left[\frac{h''}{(1 + h'^2)^{3/2}}\right]'. \tag{5}$$

We first find the solutions of (5), ignoring momentarily the boundary conditions at the contact lines, which depend on the shape of the solid surface. Due to the symmetry of (5) its solutions always have a point (the vertex) such that $h' = 0$, where we shall assume that $h = 0$ and $y = 0$ without loss of generality. Notice that the present conventions differ from those used previously [17], since we now wish to derive formulae that describe sessile as well as hanging menisci.

Introducing the dimensionless curvature at the vertex $\kappa = \lambda K(0)$ in (5) one obtains

$$\frac{\mathrm{d}y}{\mathrm{d}h} = \pm\mathrm{sign}(\kappa)\frac{1 - \frac{1}{2}\sigma h^2 - \kappa h}{\sqrt{1 - \left(1 - \frac{1}{2}\sigma h^2 - \kappa h\right)^2}}. \tag{6}$$

In this expression the $+$ ($-$) sign describes the solution for $y > 0$ ($y < 0$). In the following we shall give the results for $y > 0$, since it is obvious how to change the formulae for $y < 0$. Integrating (6) we obtain $y(h)$ as

$$y = \mathrm{sign}(\sigma\kappa)\frac{\sqrt{h(h_1 + h)(h_2 + h)(h_3 - h)}}{h_1 + h} + [\mathrm{sign}(\kappa)]^{(1-\sigma)/2} h_2 \left[\mathrm{F}(\phi|r^2) - \mathrm{E}(\phi|r^2)\right], \tag{7}$$

where $\mathrm{F}(\phi|r^2)$ and $\mathrm{E}(\phi|r^2)$ are the elliptic integrals of the first and second kind, and

$$r = h_3/h_2, \qquad h_1 = 2\sigma\kappa, \qquad h_2 = \sigma\left(\sqrt{\kappa^2 + 4\sigma} + \kappa\right), \qquad h_3 = \sigma\left(\sqrt{\kappa^2 + 4\sigma} - \kappa\right), \qquad \phi = \arcsin\sqrt{hh_2/(h_1 + h)h_3}. \tag{8}$$

By means of (7) and (8) we can describe the shape of the free surface of any cylindrical meniscus, sessile or hanging. In Fig. 2 we show some of these solutions. Notice that for $\sigma = -1$ the solutions (7) have always two symmetric inflexion points.

The free surface of the rivulet is the part of solution (7) that arrives at the substrate with the appropriate contact angles. To find this part it is convenient to write (7) in terms of the parameter $\varphi = \mathrm{sign}(\kappa)\arctan h'$; then

$$h = \zeta(\varphi) \equiv -\sigma\kappa + \mathrm{sign}(\sigma\kappa)\sqrt{\kappa^2 + 4\sigma\sin^2(\varphi/2)},$$
$$y = \eta(\varphi) \equiv \mathrm{sign}(\sigma\kappa)\Big[-\kappa\mathrm{E}(\varphi/2| - 4\sigma/\kappa^2) + (\kappa + 2\sigma/\kappa)\mathrm{F}(\varphi/2| - 4\sigma/\kappa^2)\Big]. \tag{9}$$

Here $\varphi \in [0, \pi]$ if $\sigma = 1$. For $\sigma = -1$ (see Fig. 2) we have $\varphi \in [0, \varphi_i]$, where $\varphi_i = 2\arcsin(|\kappa|/2)$ is the value of φ at the inflexion point, whose coordinates are $h_i = \kappa$ and $y_i = \eta(\varphi_i)$. Then (9) describes the solution for $0 \leq h \leq h_i$. The solution for $h_i \leq h \leq 2h_i$ is $h = 2h_i - \zeta(\varphi)$ and $y = 2y_i - \eta(\varphi)$.

Let us denote with $s(y)$ the topography of the substrate scaled by λ. Then the free surface must satisfy the boundary conditions at the left and right contact lines y_l and y_r (defined by $h(y_{l,r}) = s(y_{l,r})$), which can be written as

$$\arctan h' = \arctan s' + \sigma\theta_l \quad \text{at } y = y_l, \qquad \arctan h' = \arctan s' - \sigma\theta_r \quad \text{at } y = y_r, \tag{10}$$

using appropriate determinations of $\arctan s'$. Summarizing, the free surface is the part of solution (7) limited by y_l and y_r, and may, or may not, include inflexion points.

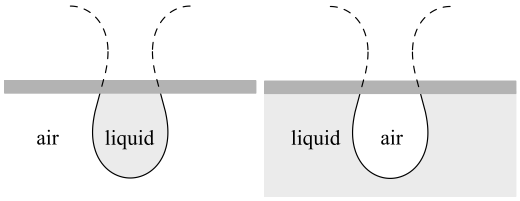

Fig. 3. The liquid may be located on either side of the curves in Fig. 2. Here we show two examples based on the curve for $\sigma = -1$ and $\kappa = 1.6$. The dark grey is the substrate, and the dashed lines are the parts of the solution that have been discarded.

Notice that each curve in Fig. 2 describes an interface between the liquid and the air. Then the same curve may represent a long filament of liquid immersed in air or a cylindrical bubble of air within a liquid, as shown in Fig. 3.

We now turn to the velocity field. We define the dimensionless stress tensor $\boldsymbol{\tau} = \mathsf{T}/\lambda\rho g \sin\alpha$. Then the conservation of linear momentum leads to

$$\partial_y \tau_{xy} + \partial_z \tau_{xz} = -1. \tag{11}$$

The boundary conditions on the solid surface and on the free surface are

$$U(y, z = s) = 0, \qquad \left(\tau_{xz} - h'\tau_{xy}\right)_{z=h} = 0. \tag{12}$$

Nothing has been said yet concerning the rheology of the liquid. In the following we shall assume that the liquid is Newtonian. Defining the dimensionless velocity $u = U\mu/\lambda^2\rho g \sin\alpha$, where μ is the viscosity, we can write Eq. (11) as

$$\partial_{yy} u + \partial_{zz} u = -1, \tag{13}$$

subject to the boundary conditions

$$u(y, z = s) = 0, \qquad \left(\partial_z u - h'\partial_y u\right)_{z=h} = 0. \tag{14}$$

The last condition implies that the isovelocity contours are perpendicular to the free surface (see Figs. 4 and 5), as already noticed by Allen and Biggin [2].

In general, problem ((13)–(14)) must be solved numerically. An exception arises when the free surface is a circular cylinder (which occurs if surface tension dominates so that $g\cos\alpha$ can be neglected in (4)), and if in addition the solid surface is a plane and the contact angles are $\pi/2$. When all these conditions are met the velocity field can be obtained in closed form [17].

To find the solution for a specific situation (say, for a given value of the volumetric flow Q) it is necessary to know $s(y)$, the contact angles $\theta_{l,r}$, which are input data, and we must find κ, that is connected in a non-trivial way to $s(y)$ and to the dimensionless cross-sectional area a of the rivulet through the integral condition

$$\int_{y_l}^{y_r} |h - s|\, \mathrm{d}y = a. \tag{15}$$

To solve the problem we follow an iterative procedure. We first guess κ. Next we compute the velocity field, and then Q. The procedure is repeated, varying κ until the specified flow is obtained

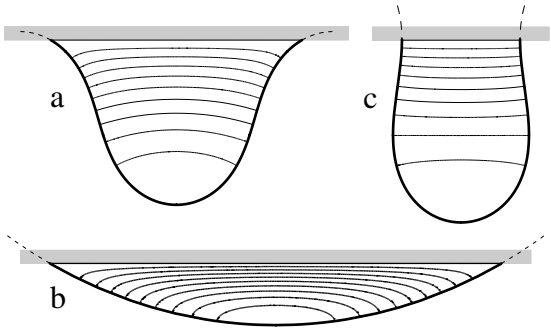

Fig. 5. Examples of hanging rivulets. (a) and (b): $\kappa = 1.2$, $\theta_l = \theta_r = 30°$; (c) $\kappa = 1.51$, $\theta_l = \theta_r = 90°$. Notice that the free surface of rivulet (b) has no inflexion points. The grey regions are the substrates, the thick lines are the free surfaces and the dashed lines are the disregarded portions of solution (7). We also show with thin lines some equally spaced isovelocity contours.

by trial an error. As examples, in Fig. 4 we show the cross section of two sessile rivulets running in wedge-shaped channels, and in Fig. 5 three rivulets hanging below a plane. In this way we can obtain the exact solutions we are seeking, but their stability must still be checked. This issue is not obvious, and will be briefly discussed later on.

3. Rivulets hanging below a plane

Since the exact solutions for rivulets over an inclined plane were already obtained [17], we investigate here rivulets hanging below such a plane, and in the following we shall assume $\theta_l = \theta_r = \theta$. We shall be interested in the global properties of the rivulet, namely, the cross-sectional area a, the dimensionless thickness $h_m = \max(h)$, the dimensionless width d of the wetted region (which may be different from the width of the rivulet; see for example Fig. 5(c)), and the dimensionless volumetric flow $q = \int u\, \mathrm{d}a$. Any other quantity of interest, such as the averaged velocity, the drag coefficient, the Reynolds number, etc., may be obtained in terms of these.

The geometrical properties of a suspended rivulet whose contact angle is θ can be easily found using the formulae of Section 2. From (9) we obtain

$$h_m = \begin{cases} \zeta(\theta), & 0 \le h \le h_i \\ 2h_i - \zeta(\theta), & h_i \le h \le 2h_i, \end{cases}$$
$$d = \begin{cases} 2\eta(\theta), & 0 \le h \le h_i \\ 2[2y_i - \eta(\theta)], & h_i \le h \le 2h_i. \end{cases} \tag{16}$$

In addition, using (15) one finds

$$a = d(h_m - \kappa) + 2\sin\theta, \tag{17}$$

an expression already obtained by Pitts [19] for suspended drops in a narrow gap.

3.1. Stability of static hanging menisci

Before considering the properties that depend on the velocity field we must say a few words about the stability of the meniscus.

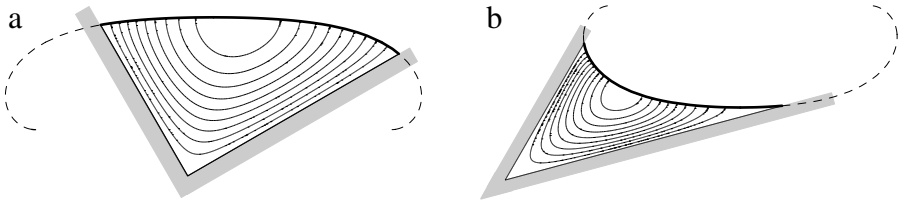

Fig. 4. Examples of sessile rivulets. (a) $\kappa = -0.05$, $\theta_l = \theta_r = 70°$; (b) $\kappa = 0.1$, $\theta_l = 40°$, $\theta_r = 10°$. The grey regions are the substrates, the thick lines are the free surfaces and the dashed lines are the disregarded portions of solution (7). We also show with thin lines some equally spaced isovelocity contours.

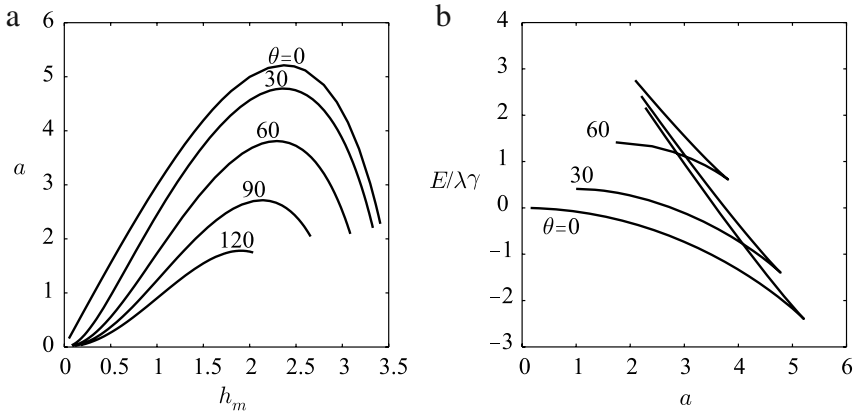

Fig. 6. (a) Area vs. height; (b) energy vs. area. Contact angles are in degrees.

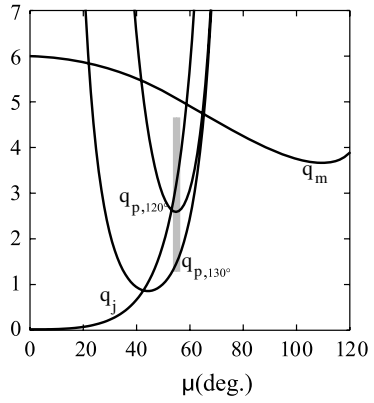

Fig. 7. Stability limits on the dimensionless volumetric flow for hanging rivulets: q_m is the limit based on the criterion of Pitts [19], and q_j and $q_{p,\alpha}$ are given by Eqs. (20) and (21) respectively. The grey vertical strip marks the range of q's investigated in the experiment reported in [20].

A hanging rivulet may be unstable with respect to perturbations of two kinds: (a) those that preserve the translational symmetry, and (b) those that tend to break the cylinder into a series of drops, or that lead to the fall-off or the ejection of drops. We shall postpone the discussion of the latter, since the stability of these modes depends on the velocity field; their detailed investigation is beyond the scope of this paper, but some comments will be given in the next section.

The stability against perturbations that preserve translational symmetry is not affected by the velocity field. Then we can apply the results of Pitts [19] for a static hanging meniscus, which we briefly recall. The plot of the dimensionless cross-sectional area of the meniscus as a function of h_m for a fixed θ (Fig. 6(a)) shows that a has a maximum, below which there are two menisci that have the same area but different h_m. It can be shown [19] that the meniscus having the larger h_m corresponds to a maximum of the total (gravitational plus surface) potential energy E per unit length of the meniscus, and therefore is unstable. In Fig. 6(b) we plot E vs. a, to identify which of the two configurations that exist for a given a corresponds to the minimum E. The maximum value of a that can be achieved for stable configurations corresponds to the maximum dimensionless volumetric flow q_m that can be attained for a given θ (provided no other instability occurs), and can be computed from the numerical solutions of ((13)–(14)). In Fig. 7 we plot $q_m(\theta)$. Note that q_m depends weakly on θ; in fact $3.65 < q_m < 6$ in the whole interval $0^\circ \le \theta \le 120^\circ$. Henceforth we shall consider only the configurations with $q \in [0, q_m]$.

Clearly the previous considerations hold for a meniscus hanging from a plane, and should be changed if the topography of the substrate is different [21].

3.2. Numerical results

To find q it is necessary to calculate the velocity field. To this end we employed a finite element method to integrate (13) subject to the boundary conditions (14), as we did previously [17]. In this reference the reader can find a discussion of the accuracy of the method. Typical results for the velocity field are shown in Fig. 5, where we have drawn contour plots of u. As expected, the larger velocity gradients are located where the isovelocity contours are nearly parallel to the plane, which occur near the substrate, and not too close to the surface of the rivulet. On approaching the free surface the isovelocity contours fan out to become perpendicular to the surface.

We solved the problem for $\theta = 0^\circ, 30^\circ, 60^\circ, 90^\circ$ and 120°. For each θ we computed solutions for a range of κ sufficient to cover the interval $10^{-4} \le q \le q_m$. The results are displayed in Fig. 8, where we plot the curvature at the vertex, the area, the width of the wetted region, and the aspect ratio h_m/d as functions of the volumetric flow, which is an easily measured quantity. From Fig. 8 any other property of interest can be obtained. Notice that the numerical results are needed only to establish the connection between q and κ, as the other parameters are given in terms of κ by the exact formulae ((16)–(17)).

As remarked by Duffy and Wilson [8], contrarily to what happens for sessile rivulets, it is possible to have hanging rivulets with $\theta = 0$. For small q the dimensionless width of these rivulets tends to the constant value 2π. On the other hand, for $\theta \neq 0$ the thickness and the width of the rivulets tend to zero for $q \to 0$, but the aspect ratio tends to a constant value (which depends on θ). The origin of this different behaviour is that for $\theta = 0$ the free surface always has inflexion points, while for $\theta \neq 0$ it does not have inflexion points if q is small. We observe that regardless of θ one has $0 \le d \le 2\pi$ for any q. Notice also that $h_m/d < 1$, except for large θ and q close to q_m.

Using Fig. 8, the properties of any hanging rivulet, for any liquid and any inclination of the plane can be obtained, because the dependence on γ, ρ, μ, g and α are implicit in the length and velocity scales. This is the advantage of this figure, which displays in compact form the properties of all possible rivulets hanging below a plane.

However, to compare the present results with actual measurements it is convenient to know the behaviour of the physical properties of a rivulet as functions of the inclination α (for fixed θ) for fixed dimensional volumetric flow Q, or vice versa, as functions of Q for fixed α. Of course these can be obtained by elaborating the data of Fig. 8, but the result is far from obvious since the length and velocity scales depend on α in a non-trivial way. For example, in Fig. 9 we show the area $A = \lambda^2 a$ of the cross section of the rivulet, as well as the Reynolds number $Re = \rho U H_m/\mu$ as functions of α,

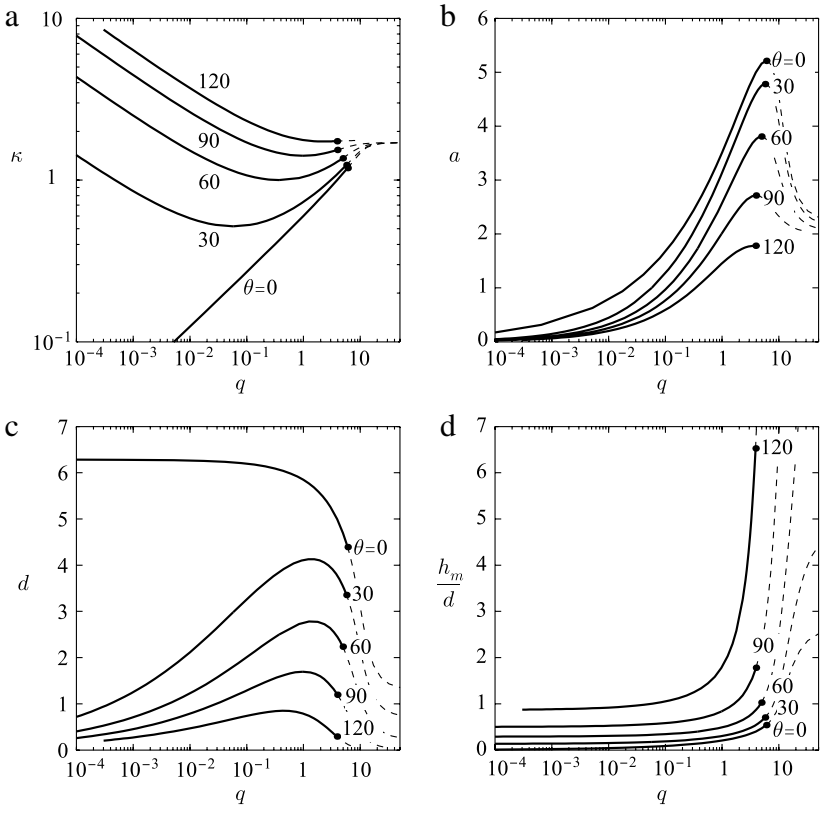

Fig. 8. Properties of hanging rivulets. (a)–(d): curvature at the vertex, cross-sectional area, width and aspect ratio h_m/d of the rivulet as functions of the volumetric flow. On each curve the dot indicates the limit of stability given by q_m and the dashed portions of the curves correspond to unstable menisci. Angles are in degrees.

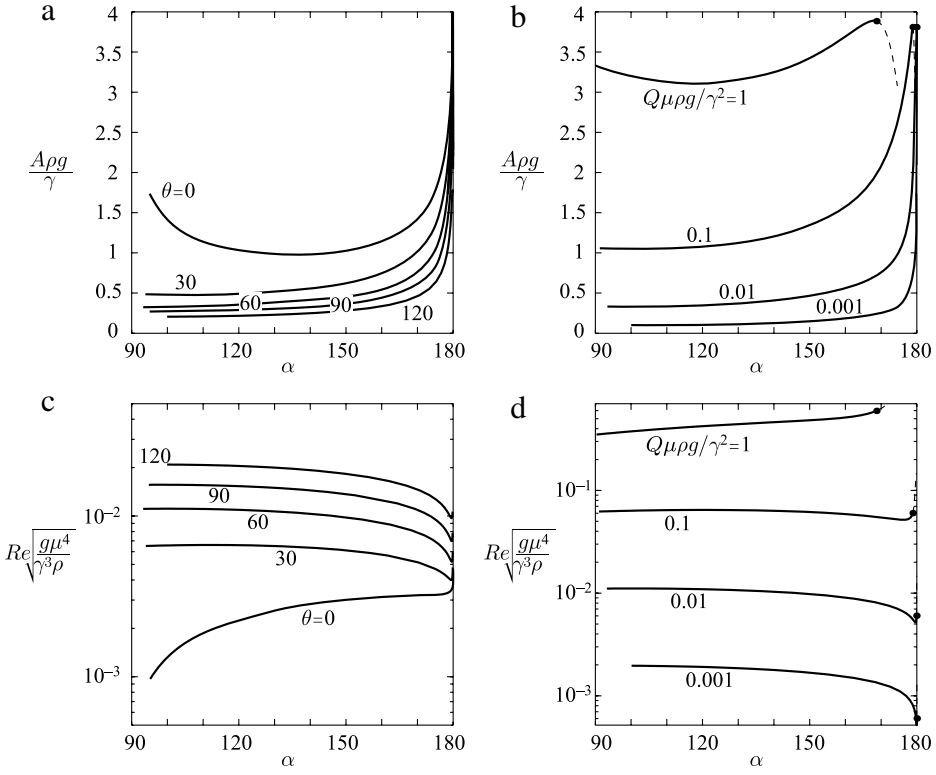

Fig. 9. Area versus α: (a) for $Q\mu\rho g/\gamma^2 = 0.01$ and different θ; (b) for $\theta = 60°$ and different Q. Reynolds number versus α: (c) for $Q\mu\rho g/\gamma^2 = 0.01$ and different θ; (d) for $\theta = 60°$ and different Q.

with Q kept constant. Clearly, the behaviour of the curves in this figure, such as the non-monotonic trend of A in some instances, as well as the weak dependence of Re on α, are not obvious from the results displayed in Fig. 8.

4. Discussion

In the present paper we have not taken into account the van der Waals forces that can be important for very thin liquid layers (≈100–1000 Å [22]). Due to these forces a static liquid layer suspended from a horizontal plane may be stable if its thickness is smaller than a critical value [23]. According to these results it can be expected that the present theory will describe correctly a rivulet whose thickness is much larger than the above-mentioned critical value, because the van der Waals forces will only affect the shape of the free surface in the neighbourhood of the contact lines.

So far we have not considered the stability of the hanging rivulets with respect to perturbations that break the translational symmetry. This is a very difficult endeavour. Drop fall-off from pendent rivulets has been investigated experimentally by Indeikina et al. [20], who also developed an approximate treatment (which excludes perfectly wetting liquids) of the instability, based on lubrication theory. For $\theta \neq 0$, and using the present notation, their theoretical results are the following: (a) if $\alpha + \theta < \pi$ (we recall that $\pi/2 < \alpha \leq \pi$) fall-off occurs by a jet mechanism if the condition

$$\cos(d/2) < -1/4 \tag{18}$$

is satisfied; (b) if $\alpha + \theta > \pi$, fall-off of drops occurs by means of a pinch-off mechanism if

$$1.5[-\cos(d/2)]^{1/6} > -\tan\alpha/\tan\theta. \tag{19}$$

These conditions mean that (for $\theta \neq 0$) drop fall-off occurs if d exceeds a critical value, which is slightly larger than π. Notice that according to Eqs. (18) and (19) if $\alpha = \pi$ the rivulet is unstable.

The experiments reported in [20] are in reasonable agreement with Eqs. (18) and (19). It should be stressed that Indeikina et al. [20] did not measure the contact angle, but used it as a fitting parameter in their theory. Thus they assumed $\theta = 55°$, corresponding to a glycerin–water solution on Plexiglas, so that the validation of the theory is limited to similar θ. We believe that these results can be taken (with caution) as a guide to assess the stability of our solutions against drop fall-off, thus indicating that the maximum volumetric flow of rivulets with a contact angle not very large may be less than q_m. In terms of q the conditions (18) and (19) can be expressed as

$$q > q_j = 1.079\tan^3\theta, \tag{20}$$

$$q > q_{p,\alpha} = \frac{4}{9}\tan^3\theta\left[1 + \frac{9}{8}\pi\left(\frac{\tan\alpha}{\tan\theta}\right)^6 L(0)^{-6}\right]. \tag{21}$$

According to Indeikina et al. [20], $L(0) = 1.5$. In Fig. 7 we have plotted q_j and $q_{p,\alpha}$ for two values of α, as well as the range of q investigated in [20]. Of course, conditions (20) and (21) cannot be taken seriously for large θ, as they were obtained by means of an approximate treatment based on lubrication theory. However, it appears from Fig. 7 that the volumetric flow is limited by q_j for small θ, by $q_{p,\alpha}$ for larger θ, and perhaps by q_m for very large θ. For fixed (but not very large) θ, q is limited by q_j for small α and by $q_{p,\alpha}$ for large α.

On the other hand Indeikina et al. [20] did not observe the Rayleigh pinching instability nor the inertial meandering instability, that occur for sessile rivulets. But it should be noticed that they did not explore the full range of Q. While the velocity gradients present in the rivulet should inhibit the growth of the Rayleigh instability, we expect this instability to occur for very small Q.

Alekseenko et al. [24] investigated the formation of waves on the surface of a rivulet hanging below an inclined circular cylinder that is irrigated by a liquid jet. They found that the waves appear at a distance L_w from the point where the jet impacts the cylinder. This distance depends on Q and α. For large α it is an increasing function of Q, but for smaller α it attains a maximum for a certain Q and then diminishes and finally vanishes for a critical volumetric flow Q^*. For $Q > Q^*$ the waves are present along the entire rivulet. It appears reasonable that a qualitatively similar behaviour will be observed for rivulets hanging below a plane. This means that in the previously mentioned unstable situations, the present theory can still be applied near the irrigation point, up to a distance of the order of L_w. Beyond this region, the presence of waves breaks the translational symmetry and the present theory cannot be applied.

The instabilities just discussed belong to the Rayleigh–Taylor (R–T) family. In the linear approximation the maximum growth rate Γ_m of the R–T instability of a uniform liquid layer of thickness H_0 below a horizontal plane [22] is $\Gamma_m = \rho^2 g^2 H_0^3/12\mu\gamma$. Although the velocity gradients present in a rivulet will tend to hinder the development of the instability, we can tentatively take Γ_m as an estimate of the order of magnitude of the maximum growth rate of the R–T instability for the rivulet (replacing g by $g|\cos\alpha|$ and H_0 by the average thickness). It is reasonable to guess that in the nonlinear regime the instability tends to produce structures whose amplitude is of the order of the wavelength. Then if the wavelength of the most unstable mode is smaller than the thickness of the rivulet we expect that the nonlinear evolution of the instability will lead to the formation of structures that travel along the rivulet but do not fall-off. On the other hand, if the wavelength is larger than the thickness we expect that the nonlinear evolution will lead to drop fall-off. The reciprocal of Γ_m gives the characteristic time for the growth of the R–T instability, which multiplied by the average flow velocity Q/A yields $L_w \approx Q/A\Gamma_m$.

5. Conclusions

We have shown how to construct solutions describing steady parallel flows with a free surface, running either above or below a solid surface whose profile in a plane perpendicular to the direction of flow is arbitrary, and whose inclination can vary from 0° to 180°. These solutions are based on a general formula from which the shape of the free surface can be obtained as soon as the profile of the substrate, the contact angles, and an additional parameter such as the curvature at the vertex are given. For a Newtonian liquid the velocity field is then obtained solving a Poisson equation in the domain defined by the cross section of the rivulet.

We next investigate rivulets hanging below an inclined plane. We calculate the shape of the free surface, the velocity field, and global properties such as the volumetric flow and various geometrical quantities. We consider several contact angles in the range 0°–120°, and dimensionless volumetric flows from 10^{-4} to q_m. The present results can also be applied when the slope of the substrate is not uniform, but varies slowly with X.

Our theory is exact so that the results we report are not limited, except by eventual instabilities. In this respect they are an improvement on those published in the literature, since the latter are based on approximations that are valid only when the slope of the free surface is small.

Acknowledgements

We acknowledge grant PICTO FONCYT/UF 21360 BID OC/AR 1728 from FONCYT and Universidad Favaloro.

References

[1] G.D. Towell, L.B. Rothfeld, Hydrodynamics of rivulet flow, AIChE J. 12 (5) (1966) 972–980.
[2] R.F. Allen, C.M. Biggin, Longitudinal flow of a lenticular liquid filament down an inclined plane, Phys. Fluids 17 (1974) 287.
[3] B.R. Duffy, H.K. Moffatt, Flow of a viscous trickle on a slowly varying incline, Chem. Eng. J. 60 (1–3) (1995) 141–146.

[4] S.V. Alekseenko, P.I. Geshev, P.A. Kuibin, Free-boundary fluid flow on an inclined cylinder, Sov. Phys. Dokl. 42 (1997) 269–272.
[5] S.K. Wilson, B.R. Duffy, On the gravity-driven draining of a rivulet of viscous fluid down a slowly varying substrate with variation transverse to the direction of flow, Phys. Fluids 10 (1998) 13.
[6] D. Holland, B.R. Duffy, S.K. Wilson, Thermocapillary effects on a thin viscous rivulet draining steadily down a uniformly heated or cooled slowly varying substrate, J. Fluid Mech. 441 (2001) 195–221.
[7] S.K. Wilson, B.R. Duffy, Strong temperature-dependent-viscosity effects on a rivulet draining down a uniformly heated or cooled slowly varying substrate, Phys. Fluids 15 (2003) 827–840.
[8] B.R. Duffy, S.K. Wilson, A rivulet of perfectly wetting fluid with temperature-dependent viscosity draining down a uniformly heated or cooled slowly varying substrate, Phys. Fluids 15 (2003) 3236–3239.
[9] S. Rosenblat, Rivulet flow of a viscoelastic liquid, J. Non-Newton. Fluid Mech. 13 (3) (1983) 259–277.
[10] S.K. Wilson, B.R. Duffy, A.B. Ross, On the gravity-driven draining of a rivulet of a viscoplastic material down a slowly varying substrate, Phys. Fluids 14 (2002) 555–571.
[11] T.G. Myers, H.X. Liang, B. Wetton, The stability and flow of a rivulet driven by interfacial shear and gravity, Internat. J. Non-Linear Mech. 39 (8) (2004) 1239–1249.
[12] J.M. Sullivan, S.K. Wilson, B.R. Duffy, Air–Blown rivulet flow of a perfectly wetting fluid on an inclined substrate, Math. Ind. 12 (2008) 774–778.
[13] J.M. Sullivan, S.K. Wilson, B.R. Duffy, A thin rivulet of perfectly wetting fluid subject to a longitudinal surface shear stress, Q. J. Mech. Appl. Math. 61 (1) (2008) 25–61.
[14] K. Mertens, V. Putkaradze, P. Vorobieff, Braiding patterns on an inclined plane, Nature 430 (6996) (2004) 165.
[15] K. Mertens, V. Putkaradze, P. Vorobieff, Morphology of a stream flowing down an inclined plane. Part 1. Braiding, J. Fluid Mech. 531 (2005) 49–58.
[16] B. Birnir, K. Mertens, V. Putkaradze, P. Vorobieff, Morphology of a stream flowing down an inclined plane. Part 2. Meandering, J. Fluid Mech. 607 (2008) 401–411.
[17] C.A. Perazzo, J. Gratton, Navier–Stokes solutions for parallel flow in rivulets on an inclined plane, J. Fluid Mech. 507 (2004) 367–379.
[18] F. Bashforth, J.C. Adams, An Attempt to Test the Theory of Capillary Action, Cambridge University Press and Deighton, Bell & Co., 1892.
[19] E. Pitts, The stability of pendent liquid drops. Part 1. Drops formed in a narrow gap, J. Fluid Mech. 59 (1973) 753–767. doi:10.1017/S0022112073001849.
[20] A. Indeikina, I. Veretennikov, H.C. Chang, Drop fall–off from pendent rivulets, J. Fluid Mech. 338 (1997) 173–201.
[21] D.H. Michael, Meniscus stability, Annu. Rev. Fluid Mech. 13 (1) (1981) 189–216.
[22] A. Oron, S.H. Davis, S.G. Bankoff, Long-scale evolution of thin liquid films, Rev. Modern Phys. 69 (3) (1997) 931–980. doi:10.1103/RevModPhys.69.931.
[23] G.V. Kolmakov, E.V. Lebedeva, A.A. Levchenko, L.P. Mezhov-Deglin, A.B. Trusov, V.B. Shikin, Stationary nonlinear waves at the surface of a thin liquid layer under inverted gravitation conditions, Low Temp. Phys. 30 (1) (2004) 58–69. doi:10.1063/1.1645156. URL: http://link.aip.org/link/?LTP/30/58/1.
[24] S.V. Alekseenko, D.M. Markovich, S.I. Shtork, Wave flow of rivulets on the outer surface of an inclined cylinder, Phys. Fluids 8 (12) (1996) 3288–3299. doi:10.1063/1.869118. URL: http://link.aip.org/link/?PHF/8/3288/1.